Articles

Flow Cytometric Analysis of Transmembrane Phospholipid Movement in Bull Sperm†

John P. Nolan,‡,§ Susan F. Magargee,§ Richard G. Posner,|| and Roy H. Hammerstedt*,§

Department of Biochemistry and Molecular Biology, The Pennsylvania State University, University Park, Pennsylvania 16802, and Department of Chemistry, Northern Arizona University, Flagstaff, Arizona 86011

Received August 22, 1994®

ABSTRACT: Fluorescent phospholipids are useful to investigate phospholipid dynamics in biological membranes. We used flow cytometry to investigate transbilayer phospholipid movement in live sperm cells. Acyl-labeled *N*-4-nitrobenzo-2-oxa-1,3-diazole (NBD) -phosphatidylcholine (-PC), -phosphatidylethanolamine (-PE), or -phosphatidylserine (-PS) were incorporated into sperm cells, and the transbilayer location was determined by extraction of probe from cell with excess bovine serum albumin (BSA) or by chemical destruction of probe by sodium dithionite. Using these methods, we have measured the head group specific outer leaflet to inner leaflet movement (flip) of the aminophospholipids NBD-PS and NBD-PE. The fluorescent phospholipids moved inward across the plasma membrane with half-times of 1.8, 2.5, and 11.2 min, for NBD-PS, NBD-PE, and NBD-PC and reached apparent equilibrium levels of 88%, 94%, and 32% inside, respectively. The inward movement of NBD-PE was inhibited by sulfhydryl reagents, elevated intracellular Ca^{2+}, and depletion of cellular ATP. Analysis of the kinetics of NBD-PE and -PS extraction by BSA allows determination of the rates for outward movement (flop) across the plasma membrane. Half-times for flop were 4.7 and 4.5 min for NBD-PS and -PE, respectively. Based on these measurements, a simple model of NBD-phospholipid equilibria was developed and fit to the kinetic data. Computer-generated fits reflected major features of the experimental data and provide a potential tool for predicting the dynamics of endogenous lipids.

Fluorescent phospholipids are useful to investigate the lateral, transverse, and intermembrane diffusion of phospholipids in the membranes of living cells. Acyl-labeled *N*-4-nitrobenzo-2-oxa-1,3-diazole (NBD)[1] phospholipid analogues are slightly water soluble and are readily incorporated into the outer leaflet (OL) of the cell plasma membrane (PM). After incorporation, these phospholipids may move (flip) from the PM OL to the inner leaflet (IL) by passive diffusion and/or active transport [see Devaux (1991) for a review of transmembrane movement of phospholipids in cells]. Once on the PM IL, probe can diffuse through the cytoplasm to intracellular membranes (IM; mitochondrial, golgi, nuclear, etc.) or move (flop) back to the PM OL. Fluorescence microscopy can detect accumulation of probe in intracellular organelles of individual cells (Struck & Pagano, 1980; Martin & Pagano, 1987; Koval & Pagano, 1989; Kobayashi & Arakawa, 1991), but quantitation is difficult and distinction between membrane leaflets is not possible. Probe located on the OL can be rapidly extracted by excess bovine serum albumin (BSA) (Connor & Schroit, 1990; Colleau et al., 1990; Williamson et al., 1992) or chemically reduced to a nonfluorescent form by sodium dithionite (DT) (McIntyre & Sleight, 1990). Application of these methods to the study of cell populations in cuvettes has enabled quantitative estimation of OL probe.

All such cell population studies have the common limitations of (a) limited temporal resolution (>5 min) due to the need to wash away excess probe and reagents prior to measurement, (b) dependence of cuvette fluorescence measurements on a separate quantitative estimate of cell number, and (c) unknown contribution of dead or damaged cells to the population average. We describe the use of flow cytometry to address these limitations and report herein an aminophospholipid translocase (flippase) assay based on direct measurement of fluorescence of individual cells. Flow cytometry enables direct measurement of NBD-phospholipid incorporation into cells and extraction by delipidated BSA and allows evaluation of NBD-phospholipid movement between membrane surfaces in intact cells.

MATERIALS AND METHODS

Materials. 1-Acyl-2-C6-NBD-phosphatidylcholine (-PC), -phosphatidylethanolamine (-PE), and -phosphatidylserine (-PS) were purchased from Avanti Polar Lipids (Birmingham,

† This work was supported by NIH Grant HD13099 and DOE LDRD X195.

* Author to whom correspondence should be addressed.

‡ Current address: National Flow Cytometry Resource, Life Sciences Division, LS-1, M-888, Los Alamos National Laboratory, Los Alamos, NM 87545.

§ The Pennsylvania State University.

|| Northern Arizona University.

® Abstract published in *Advance ACS Abstracts,* March 15, 1995.

[1] Abbreviations: NBD, *N*-4-nitrobenzo-2-oxa-1,3-diazole; PC, phosphatidylcholine; PE, phosphatidylethanolamine; PS, phosphatidylserine; BSA, bovine serum albumin; OL, outer leaflet; PM, plasma membrane; IL, inner leaflet; DT, sodium dithionite; IM, intracellular membranes; PDA, pyridyldithioethylamine; TALP, Tyrode's buffer with albumin, lactate, and pyruvate; PrI, propidium iodide; RT, room temperature; TLP, Tyrode's buffer with lactate and pyruvate.

0006-2960/95/0434-3907$09.00/0

AL). NBD-PS was also prepared from NBD-PC by phospholipase D catalyzed base exchange in the presence of L-serine (Juneja et al., 1989) and purified by HPLC with a LC-Si column (Supelco; Bellefonte, PA) using acetonitrile/methanol/water (50/45/6.5) as the mobile phase. Pyridyldithioethylamine (PDA) was synthesized and purified by 2× crystallization from ethanol/diethyl ether (Connor & Schroit, 1988). BSA (Fraction V, ICN) was delipidated by extraction with $CHCl_3$/MeOH (2/1). 4-Br-A23187 was purchased from Molecular Probes (Eugene, OR).

Sperm Cell Preparation. Ejaculated bull sperm were washed from seminal plasma by two cycles of centrifugation (300*g* for 8 min) and resuspension in modified Tyrodes solution containing lactate, pyruvate, and 1 mg/mL BSA (TALP) at a concentration of 5×10^8 cells/mL (Nolan et al., 1992). Cells were depleted of endogenous ATP by resuspension in glucose free media and incubation with 4 μM antimycin A and 4 μM rotenone for 30 min at 37 °C. For experiments involving calcium ionophore (17 μM) and PDA (4 mM), cells were treated for 5 min before measurement.

Flow Cytometry of Sperm Cells. Sperm cell fluorescence was measured on an EPICS VII Flow Cytometer (Coulter Corp., Hialeah, FL). Cell associated fluorophores were excited at 488 nm (100 mW). NBD fluorescence was measured through a 590 nm long-pass dichroic mirror and 525 nm band-pass filter. Propidium iodide (PrI) fluorescence was measured through the same dichroic mirror and a 610 nm long-pass filter. Sperm cells were identified on the basis of forward angle and 90° light scatter. Dead cells were excluded from analyses based on PrI fluorescence. FITC-microbead standards (Flow Cytometry Standards Corp., Research Triangle Park, NC) were routinely run to assess day-to-day variations in instrument performance. Depending on experimental design, data were acquired in one of two modes: collection of discrete histograms at each time point (maximum throughput/temporal resolution = 1 min/measurement) or continuous measurement using time as a parameter (temporal resolution = 25 s/measurement). Changes in sperm cell fluorescence were measured continuously by collecting data in list mode. List mode files were analyzed on Elite software (Coulter Electronics Corp.) to produce two parameter histograms (log NBD fluorescence vs time). Histogram data were arrayed by the program 64 × 64 (Writehand Man, Inc., Cooper City, FL), and the mean NBD fluorescence channel number was calculated for each time channel by a custom developed Basic routine (courtesy of Michael Hogan). For all histograms acquired, the mean channel number was converted to linear scale before subtraction of the background signal determined for unlabeled cells.

Kinetic Assay of NBD-Phospholipid Movement. NBD-phospholipids (0.1 nmol/mL of sperm in <1% (v/v) ethanol) were added to sperm cells (1×10^7/mL) in Tyrode's with lactate and pyruvate but no BSA (TLP) at RT (21−24 °C). Preliminary experiments found that ethanol injection provided more rapid and complete probe incorporation than the use of PC vesicles as a carrier. At 1 min after probe addition, and 2 min intervals thereafter, 25 μL aliquots were transferred to either 225 μL of TLP buffer or 225 μL of 5% delipidated BSA at 37 °C to extract OL probe. Cells diluted in buffer only were analyzed immediately (to give the population mean total cell associated NBD-phospholipid fluorescence) while cells diluted into buffer +5% BSA were analyzed after 5 min (representing cell associated NBD-phospholipid after OL extraction). Alternately, OL probe was quenched by addition of 20 mm DT and read after 1 min. This experimental design allowed a maximum temporal resolution of 2 min/sample (two measurements/sample, 1 min/measurement).

Data Analysis and Computer Modeling. Kinetic data were analyzed by nonlinear curve fitting (Sigmaplot, Jandel Scientific, Corta Madera, CA). NBD-phospholipid extraction data (Figure 2A) were fit to single-exponential [$F(t) = A\ e^{-k_1 t} + B$] or double-exponential [$F(t) = A(1 - e^{-k_1 t}) + B(1 - e^{-k_2 t}) + C$] equations, where $F(t)$ is the mean cellular fluorescence at time t. Phospholipid flip kinetic data (Figures 3 and 4) were fit to single-exponential [$F(t) = A(1 - e^{-k_1 t}) + B$] or double-exponential [$F(t) = A(1 - e^{-k_1 t}) + B(1 - e^{-k_2 t}) + C$] equations, where $F(t)$ is the fraction of total cellular label not extracted by BSA after 5 min. Half-times were calculated as $T_{1/2} = \ln 2/k$.

Composite data (Figure 6) were fit to simultaneous differential equations defining a model of phospholipid equilibria (Figure 5):

$$\text{free probe} = \text{total probe} - \text{dOL} - \text{dIL} - \text{dIM}$$

$$\text{dOL}/dt = k_{\text{incorp}}(\text{free probe}) - k_{\text{extract}}\text{OL} - k_{\text{flip}}\text{OL} + k_{\text{flop}}\text{IL}$$

$$\text{dIL}/dt = k_{\text{flip}}\text{OL} - k_{\text{flop}}\text{IL} - k_{\text{diff}}\text{IL}$$

$$\text{dIM}/dt = k_{\text{diff}}\text{IL}$$

where at $T = 0$, free probe = total probe, and OL, IL, and IM = 0. Incorporation of added NBD-phospholipid into the PM OL was modeled as a first-order process, and rate constants (k_{incorp}) were estimated from the half-times of incorporation (Figure 1). Phospholipid movement between the PM OL and PM IL and between the PM IL and internal membranes (IM) were modeled as first-order processes. Transbilayer movement (PM OL to PM IL) was defined as reversible, while intermembrane movement (PM IL to IM) was assumed to be essentially irreversible on the time scales involved here. Rate constants for outward (k_{flop}) and inward (k_{flip}) transbilayer movement were estimated from exponential curve fits to the data in Figures 2 and 3, as described above. Rate constants for NBD-phospholipid extraction by BSA (k_{extract}) and intracellular diffusion (k_{diff}) were estimated as being pseudo-first-order and similar to that for incorporation, since these processes are expected to have a similar dependence on phospholipid head group.

RESULTS

Incorporation of NBD-Phospholipids into Sperm. Fluorescent phospholipid analogues were rapidly incorporated nto the sperm PM by addition of analogue (in ethanol) to a sperm suspension. For all lipids tested, the fluorescence histograms were unimodal, but the kinetics and extent of NBD-phospholipid incorporation varied with the phospholipid head group (Figure 1). When added to the sperm cell suspension in equal amounts, 2−5 times more NBD-PE was incorporated than either NBD-PS or NBD-PC. The kinetics of incorporation were markedly slower for NBD-PS (estimated $T_{1/2} > 10$ min) as compared to NBD-PE and NBD-PC ($T_{1/2} < 5$ min). Sperm NBD-PC fluorescence reproducibly decreased after reaching a maximum approximately 10

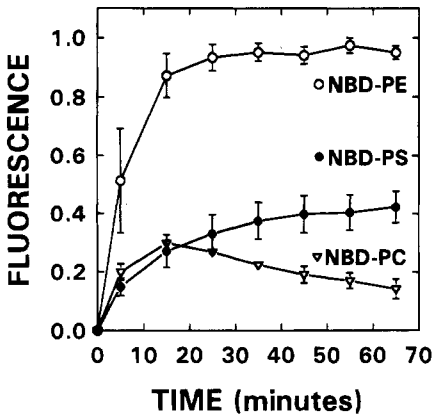

FIGURE 1: Incorporation of NBD-phospholipids into sperm cells. NBD-phospholipids (NBD-PE, ○; NBD-PS, ●; NBD-PC, △) were added to sperm (0.10 nmol/10^7 cells, in <0.5% EtOH) in TLP buffer and cellular fluorescence measured as described in Materials and Methods. Data represent the average and standard error (SEM) of four experiments.

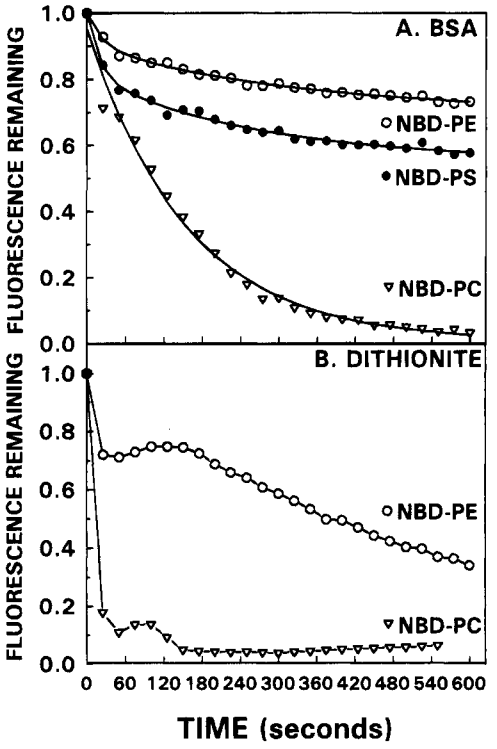

FIGURE 2: (A) Extraction of NBD-phospholipids from sperm. NBD-phospholipids (NBD-PE, ○; NBD-PS, ●; NBD-PC, △) and sperm were incubated for 10 min as in Figure 1 and then diluted 10-fold into buffer plus 5% BSA. Data represent the average of 2−4 experiments. (B) Quench of NBD-phospholipids by dithionite. Cells were labeled with NBD-phospholipids (NBD-PE, ○; NBD-PC, △) for 10 min, followed by the addition of 20 mM DT. Data presented are representative of 2−4 separate determinations.

min after addition, indicating that cellular probe may be in equilibrium with unknown extracellular pools.

Extraction of NBD-Phospholipids from Sperm. The slightly water soluble fluorescent phospholipids were extracted from sperm by addition of excess delipidated BSA. This extraction was measured as a decrease in sperm cell fluorescence (Figure 2A). Addition of BSA alone increased the fluorescence of unlabeled cells; therefore, this background was subtracted from fluorescence values of BSA treated sperm. At 10 min after probe addition virtually all of the cellular NBD-PC was extracted by 5% BSA. Extraction of NBD-PC by BSA was well fit by a single-exponential equation [$F(t) = A\ e^{-k_1 t} + B$] with a calculated $T_{1/2}$ of 108 s. The extraction kinetics for NBD-PE and NBD-PS exhibited a rapid initial decrease in cell fluorescence, followed by a slower decrease. A fraction of cellular NBD-PE and NBD-PS fluorescence was not extracted even at long times after BSA addition. Complete interpretation of NBD-phospholipid extraction kinetics will be presented below.

Table 1: Calculated Rate Constants for Outward Movement (Flop) of NBD-Phospholipids

NBD-phospholipid	$T_{1/2}$ (min)[a]
NBD-PC	
NBD-PE	5.6 ± 0.9 (9)
NBD-PS	5.6 ± 1.4 (6)

[a] Calculated from double-exponential fits to the extraction data as shown in Figure 2A. Presented are the means ± SEM of (n) determinations.

Quench of NBD-Phospholipid Fluorescence by Dithionite. Labeled cells were treated with sodium dithionite (DT), which reduces the 7-nitro group of the NBD moiety to an amine and destroys the fluorescent properties of the probe (McIntyre & Sleight, 1991), to provide an alternate means of determining the exofacially located fraction of fluorescent phospholipid. When 20 mM DT was added to cells prelabeled with NBD-phospholipid for 10 min, 76% (±5%, SEM; n = 5) of the NBD-PC fluorescence was quenched within 1 min of DT addition (Figure 2B). Only 26% (±5%; n = 8) of the NBD-PE fluorescence was quenched in the same interval, with the remaining fraction disappearing at a slower rate. DT quench kinetics of NBD-PS exhibited an initial decrease in cell fluorescence, followed by an unexpected fluorescence increase, before finally decreasing once more. An explanation for this apparently anomalous behavior eludes us at this time, and the phenomenon requires further investigation.

Interpretation of Extraction/Quench Data. The subcellular location of the NBD-phospholipids can be deduced from the kinetics of probe extraction by BSA and quench by DT. The extraction kinetics of NBD-PE and NBD-PS reveal three pools of lipid analogue: a rapidly extracted pool, a slowly extracted pool, and a very slowly (or non-)extracted pool. These kinetics are well fit by a double-exponential equation, $F(t) = A\ e^{-k_1 t} + B\ e^{-k_2 t} + C$. The simplest interpretation of this data is that PM OL probe (pool A) is rapidly extracted (with rate constant k_1), PM IL probe (pool B) must move to the OL before extraction (with rate constant k_2), and the nonextracted fraction (pool C) has diffused from the PM IL to internal organelle membranes. NBD-PC is extracted in a single kinetic phase indicating that most of the probe is on the PM OL or that movement from the IL to the OL is faster than extraction. Dithionite quench kinetics show that most NBD-PC is quenched rapidly, confirming an OL location for this analogue. Quenching of NBD-PE reveals two pools: a rapidly quenched fraction, corresponding to OL probe, and a slowly quenched fraction, representing either DT leakage into the cell or NBD-PL movement back to the OL. This confirms our interpretation of the BSA extraction kinetics and means that the second, slow phase of extraction of NBD-PE and NBD-PS (rate constant k_2) represents a measurement of outward movement (flop) of lipid. The half-times calculated for flop of NBD-PS and NBD-PE across the plasma membrane are presented in Table 1. As measured

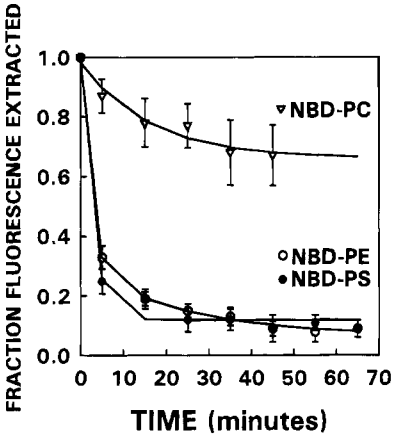

FIGURE 3: Kinetics of NBD-phospholipid flip across the PM. NBD-phospholipids (NBD-PE, ○; NBD-PS, ●; NBD-PC, △) were added to sperm as described in Figure 1 at RT. At the indicated times, aliquots were diluted 10-fold into TLP only and TLP + 5% BSA. Samples diluted in TLP only were read immediately to determine total cellular fluorescence. Cells diluted into TLP+BSA were read after 5 min. The difference between these values, divided by the total cellular fluorescence at time of sampling, represents the fraction of probe bound to the cell that could be removed at time *t*. Shown are the means (±SEM) of at least three separate experiments. Lines represent exponential fits to the data.

Table 2: Outside−Inside Transbilayer Movement (Flip) of NBD-Phospholipids

NBD-phospholipid	fraction flipped[a]	$T_{1/2}$ (min)[b]
NBD-PC	0.32	11.2
NBD-PE	0.94	2.5
NBD-PS	0.88	1.8

[a] Obtained from the results of exponential curve fits to data in Figure 3. [b] Calculated from the results of curve fits to the data in Figure 3.

here, the size of the PM IL pool, and thus the rate of flop, is affected by the rates of flip (PM OL to IL) and diffusion from the IL to internal membranes. Thus, the values calculated represent a lower limit on the outward movement of NBD-phospholipids across the PM.

Kinetics of NBD-Phospholipid Flip. The ability of BSA to extract NBD-phospholipids from cells was used to determine the kinetics of NBD-phospholipid transbilayer flip. Cells were labeled with NBD-phospholipids, and at intervals aliquots were extracted with BSA at 37 °C for 5 min. The time course of movement of NBD-phospholipid from a rapidly BSA-extracted pool (probe associated with the OL) to a slowly extracted pool (probe associated with the IL) is presented in Figure 3. The majority of NBD-PE and NBD-PS rapidly became nonextractable, while most NBD-PC remained in a readily extracted pool. The calculated half-times from single-exponential curve fits [$F(t) = A\ (1 - e^{-k_1 t}) + B$] for movement of NBD-PS and NBD-PE to a slowly extracted pool were 1.8 and 2.5 min, respectively, while the half-time for flip of NBD-PC was 11.2 min. The size of the OPM pool, and thus the observed flip kinetics, reflects the rate of flip, plus a negative contribution from flop, which in turn is affected by diffusion to internal membranes. The estimated half-times of movement and apparent equilibrium distribution values for each NBD-phospholipid are presented in Table 2.

Inhibition of NBD-Aminophospholipid Flip. The head group specific flip of NBD-phospholipids across the sperm PM was inhibited by several compounds reported to inhibit

Table 3: Inhibition of Transbilayer NBD-PE Movement

	fluorescence remaining[a]	
treatment	NBD-PC	NBD-PE
control	0.24 ± 0.05 (5)	0.74 ± 0.05 (8)
4 μM 4-Br-A23187	0.10 ± 0.07 (3)	0.10 ± 0.03 (4)
4 mM PDA	0.14 ± 0.08 (3)	0.22 ± 0.05 (6)

[a] Cells were labeled with NBD-phospholipids for 10 min, followed by treatment with 20 μM sodium dithionite for 1 min. Data are the means ± SEM of (*n*) determinations.

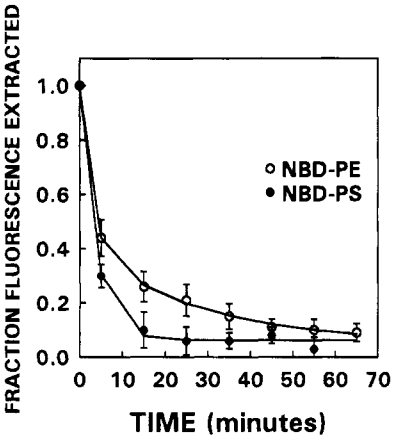

FIGURE 4: Inhibition of the aminophospholipid flippase. Sperm cells were treated with 4 μM antimycin A and 4 μM rotenone for 30 min in glucose-free media at 37 °C. NBD-phospholipids were then added (NBD-PE, ○; NBD-PS, ●; NBD-PC, △) and transbilayer phospholipid movement measured as in Figure 3. Data are the means (±SEM) of 5−7 experiments, and the lines represent exponential fits to the means.

the aminophospholipid translocase in other cell types, including sulfhydryl reagents and calcium ionophore. Pretreatment of cells with 4 mM pyridyldithioethylamine (PDA) or 17 μM 4-Br-A23187, which elevates intracellular free Ca^{2+} (Nolan et al., 1992), reduces the nonquenchable fraction of NBD-PE after 10 min to levels comparable with NBD-PC (Table 3). Partial replicates using *N*-ethylmaleimide indicate that this sulfhydryl reagent also inhibits translocase activity (data not presented).

Depletion of cellular ATP by treatment of sperm cells with antimycin A and rotenone in the absence of glucose also decreased the rate of inward movement of NBD-PE ($T_{1/2}$ = 3.7 min; Figure 4), but not the final equilibrium value. ATP depletion by this method had no measurable effect on NBD-PS movement. Müller et al. (1994) recently used 2-deoxyglucose and azide to reduce ATP levels in ram sperm by 95% and showed inhibition of both spin labeled PE and PS transport. Calvez et al. (1988) demonstrated that, in the erythrocyte, transport of spin-labeled PE is more sensitive to cellular ATP levels than transport of PS. Antimycin A plus rotenone treatment in the absence of glucose represents starved cells (no glycolytic substrates and inhibited mitochondrial function) where ATP is depleted by endogenous ATPases of all sorts. In sperm, 2-deoxyglucose is actively phosphorylated and dephosphorylated (Hiipakka & Hammerstedt, 1978). Thus, treatment with azide plus 2-deoxyglucose minus glucose constitutes a system with no glycolytic or mitochondrial metabolism, plus an additional ATP consuming process. This would be expected to deplete cellular ATP even faster. We did not measure cell ATP content in this study, but presumably antimycin A + rotenone treatment

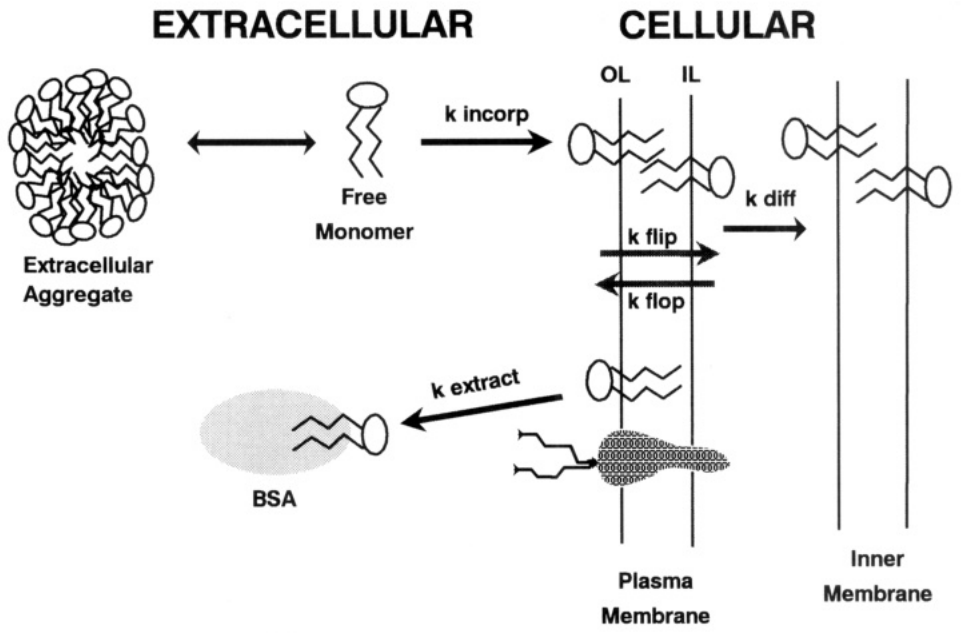

FIGURE 5: Model of NBD-phospholipid equilibria.

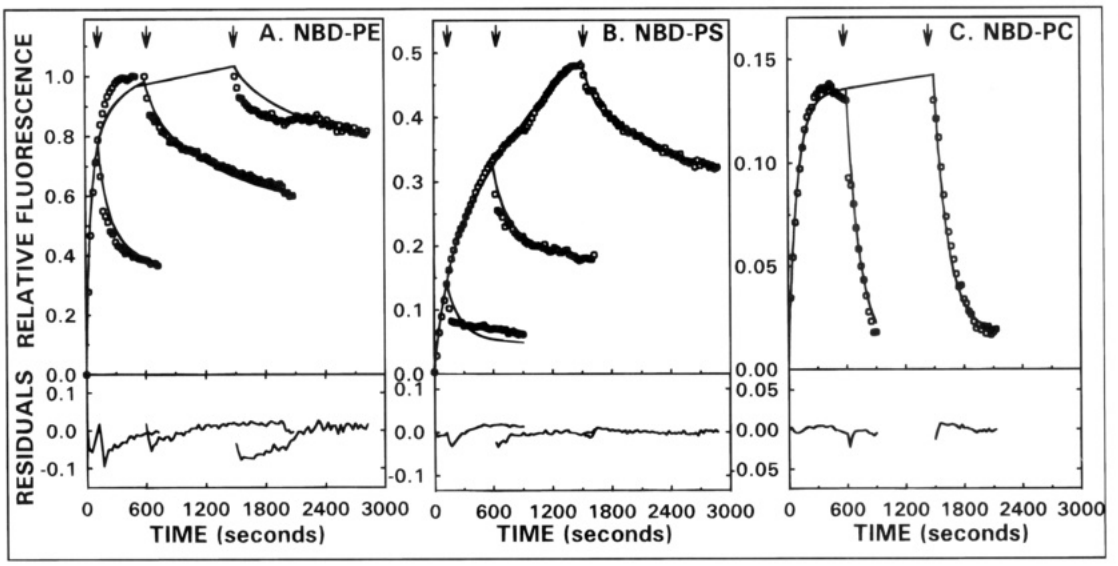

FIGURE 6: Computer modeling of composite data of NBD-phospholipid movement. Data points (circles) describing incorporation of NBD-phospholipids (A, NBD-PE; B, NBD-PS; C, NBD-PC) and extraction (arrows) at 125, 600, and 1500 s. Incorporation kinetics are representative of at least three separate measurements, while extraction kinetics are the averages of 2−4 experiments. Lines represent the results of the computer generated curve fits. Residuals are shown in the lower panels.

reduced ATP to an intermediate level compared to azide plus 2-deoxyglucose, such that PE transport was affected, but not PS transport.

Modeling of Phospholipid Movement in Sperm Cells. Because the kinetics of NBD-phospholipid movement observed above are the result of several parallel processes, the rate of any single process is difficult to determine. To obtain estimates of the rates of individual steps, a model of cellular membrane pools was developed (Figure 5) and simultaneous differential equations defining the model were fit to the composite data in Figure 6. Incorporation of added NBD-phospholipid into the PM OL was modeled as a first-order process, and rate constants were estimated from the half-times of incorporation (Figure 1). Phospholipid movement between the PM OL and PM IL and between the PM IL and internal membranes (IM) were modeled as first-order processes. Transbilayer movement (PM OL to PM IL) was defined as reversible. Intermembrane movement (PM IL to IM) was modeled to be irreversible, in view of the BSA extraction data, which shows a time-dependent increase in a non- (or very slowly) extractable fraction. This simplification is supported by consideration of the multilayered arrangement of sperm membranes. Probe which diffuses from the IPM to the OL of the outer acrosomal membrane may then flip across this membrane and diffuse to the OL of the inner acrosomal membrane. Below the inner acrosomal membrane is the nuclear membrane. Similar fates are possible for probe diffusing to the OL of the outer mitochondrial membrane. If the rates of inward movement are greater than the rates in the reverse direction, some probe may appear to be trapped inside the cell when the equilibrium is suddenly shifted, as by the addition of excess BSA. It is very difficult to assess such movements, but we assume internalized probe becomes kinetically trapped on the time scales involved here. This assumption is justified by the fact that making this step reversible did not improve the fits

Table 4: Computer Modeling of NBD-Phospholipid Movement in Sperm Cells[a,b]

	NBD-PE		NBD-PS		NBD-PC	
	initial	fit	initial	fit	initial	fit
k_{incorp}	0.0037	0.0157	0.0011	0.0017	0.0029	0.0041
$k_{extract}$	0.0037	0.0057	0.0011	0.0052	0.0029	0.0071
k_{flip}	0.0045	0.0040	0.0062	0.0021	0.0012	0.0002
k_{flop}	0.0026	0.0008	0.0031	0.0003	0.0001	0.0247
k_{diff}	0.0037	0.0006	0.0011	1×10^{-6}	0.0029	0.0379

[a] Initial estimates were made and modeling performed as described in Materials and Methods. [b] Rate constants have units of s^{-1} M^{-1} (k_{incorp}) or s^{-1} (others).

to the data as judged by the sum of squares. Rate constants for outward and inward transbilayer movement were estimated from exponential curve fits to the data in Figures 2A and 3, as described in Materials and Methods. Rate constants for NBD-phospholipid extraction by BSA and intracellular diffusion were modeled as pseudo-first-order, the acceptor species being in excess. Initial estimates were the same as for incorporation, since these processes are expected to have a similar dependence on phospholipid head group. The result of the fits are shown as lines in Figure 6 and are summarized in Table 4. Changing the initial estimates by an order of magnitude did not improve the fits as assessed by the sum of squares. Evaluation of the residuals indicated deviation of the fits from experimental values was associated primarily with the incorporation and the rapid extraction phase. This is understandable, since incorporation is likely more complex than the first-order process modeled here, and the rapid extraction was too fast to be measured well by flow cytometry. Half-times for incorporation (0.7, 2.8, 6.8 min for NBD-PE, -PC, and -PS, respectively) and flip (2.9 and 5.8 min for NBD-PE and -PS) calculated from the results of the fit were of the same order as the experimentally observed kinetics; however, for flop and internal diffusion, calculated half-times were much longer than those observed. We view the rates estimated from the modeling with caution, and possible reasons for the discrepancies between the experimental data and the resulting fits will be discussed below. Overall, computer generated fits reflect major features of the experimental data and support the general model, while identifying points for further refinement in the model and experimental methods.

DISCUSSION

This report addresses the incorporation, transbilayer movement, and subcellular localization of fluorescent phospholipids in live sperm cells. Flow cytometry is especially well suited to these studies because it measures only cell-associated fluorescence, without the need to wash away excess reagents or extracellular fluorescent probe. This allows improved accuracy and precision as well as increased temporal resolution as compared to cuvette measurements of steady-state cellular fluorescence. Flow cytometry is used here to investigate the transbilayer movement of NBD-phospholipid analogues in bull sperm. The data presented support the following model of NBD-phospholipid equilibria (Figure 5). Upon addition to the sperm sample as free monomers in ethanol, NBD-phospholipids incorporate into the sperm cell PM OL, self-assemble into extracellular aggregates (micelles or bilayer vesicles), or both, depending on the physical properties of the lipid being tested. After incorporation into the PM OL, probe can then flip to the IL. Once on the IL, probe may either flop back to the OL or diffuse through the aqueous phase to intracellular membranes (mitochondrial, acrosomal, nuclear). These movements of fluorescent phospholipids were measured using flow cytometry and rate constants were estimated using a model of phospholipid equilibria.

Incorporation of NBD-Phospholipids into Sperm Cells. The kinetics and extent of NBD-phospholipid incorporation into sperm cells varies with phospholipid head group. This is expected due to the unique properties of self-association, aqueous solubility, and affinity for the sperm PM OL of each phospholipid. Although the solubility properties and phase behavior of NBD-phospholipid species have not been extensively investigated, analogy to existing data on related species (King & Marsh, 1987) predicts a variation with head group composition. The critical micelle concentrations for spin-labeled phospholipids varied over an order of magnitude (PS > PC > PE) in the concentration range typically used in cell measurements. The kinetics of NBD-phospholipid incorporation are indicative of extracellular aggregates in dynamic equilibrium with the sperm PM OL. NBD-PE exhibits a single kinetic phase of incorporation with a $T_{1/2}$ of approximately 3 min. NBD-PC fluorescence exhibits a similar rapid increase, followed by a slower decrease in cell fluorescence. The slow incorporation kinetics of NBD-PS (Figure 1) indicate some extracellular pool (aggregate) which equilibrates with the sperm over several minutes. The slow efflux of NBD-PC from sperm after an initial maximum suggests equilibration with a stable extracellular pool of lipid. Not all added probe is sperm associated, however. When cells were labeled at identical probe/cell used for flow cytometry, pelleted by centrifugation, and the pellet and supernatant fluorescence measured in the presence of 1% Triton X-100, only 34% of NBD-PC and 57% of NBD-PE were associated with the sperm pellet 20 min after addition. Probe remaining in the supernatant might be associated with membrane fragments or other debris or may exist as vesicular aggregates. These differences in NBD-phospholipid incorporation kinetics are an example of the usefulness of flow cytometry for making measurements of cell fluorescence. The ability of flow cytometry to distinguish cellular probe from free probe provides information which is lost in bulk measurements of cell fluorescence in cuvettes. It is clear from these data that the common assumption of complete, rapid, and irreversible probe incorporation into cells may not be justified, and that such an assumption compromises quantitative interpretation of these types of studies. Another explanation for the observed decrease in cell NBD-PC fluorescence could be NBD self-quenching. Concentration-dependent self-quenching of *N*-NBD-PE in egg PC large unilamellar vesicles becomes significant at probe levels above 10 mol % (C. Aurell-Wistrom, personal communication). The surface area of a bull sperm is 145 μm^2 (Drevius, 1972) and the protein/phospholipid ratio of the anterior head PM is 0.66 (Parks et al., 1987). Assuming this value applies to the entire sperm plasma membrane and that mass is distributed equally between the two membrane leaflets, the total phospholipid surface area on the outer leaflet of the PM is approximately 96 μm^2. Further assuming an average surface area of 0.6 nm^2/phospholipid molecule on the bilayer, this amounts to approximately 1.6×10^8 phospholipid molecules. We added

about 6×10^6 molecules of NBD-PC per cell, 34% of which became cell associated. This leads to an estimate of 2×10^6 NBD-PC molecules/cell. If all of this were on the outer surface, it would represent less than 2 mol % of the total outer leaflet phospholipid. Thus, on the basis of these order of magnitude calculations, self-quenching is not likely to be an issue in the absence of significant clustering or domain formation by added probe. Whole cell measurements by flow cytometry cannot rule out such clustering, and fluorescence microscopy may be useful to address this issue.

Subcellular Localization of NBD-Phospholipids. Flow cytometry is uniquely capable of distinguishing cell associated probe from free probe, but the subcellular location of that probe is more difficult to determine. The OL of the PM is the most logical location for measured probe immediately after addition, since NBD fluorescence is greatly enhanced by a hydrophobic environment (Chattopadhyay, 1990). Extracellular aggregates adsorbed to the cell surface and not incorporated into the bilayer are expected to be self-quenched (Chattopadhyay, 1990) and therefore would not contribute to cellular fluorescence. Once inserted into the PM OL, NBD-phospholipids may move to other cellular membrane pools. To address the question of subcellular localization of fluorescent phospholipids, the fraction of cellular probe present in the OL was estimated by two different methods, extraction of probe with BSA and chemical quench of probe by dithionite. The excellent kinetic resolution of flow cytometry reveals distinct pools of cellular probes.

Extraction of NBD-Phospholipids by BSA. A fraction of cell associated NBD-phospholipid was extracted with excess BSA (Figure 2A). The kinetics of this process reflects the rate of probe transfer from the OL to excess acceptor (BSA) in solution, as well as the rate of movement of internal probe to the OL. The first phase reflects transfer from the PM OL to BSA in solution, is dictated by the physical features of the lipid, and is expected to vary with phospholipid head group (Homan & Pownall, 1988). The second step, movement from the PM IL to the PM OL (flop), reflects passive diffusion across the membrane plus any facilitated movement. A third process which may affect the measured extraction kinetics is the exchange of probe between the PM IL and intracellular membranes. This intracellular diffusion is analogous to intermembrane transfer and this rate, like the rate of extraction from the OL, is expected to vary with lipid head group. The large nonextractable fraction of NBD-PE and NBD-PS (Figure 2A) indicates that such interbilayer exchange is significant in sperm cells.

Dithionite Quench of NBD-Phospholipids. Chemical quench of OL probe by DT provides another method to address subcellular probe location. Like BSA extraction, dithionite quench of sperm cell NBD fluorescence also exhibits biphasic kinetics (Figure 2B), although the interpretation of the data is somewhat different. In this case, the initial rapid phase of decreased fluorescence reflects the destruction of PM OL probe, with the more slowly quenched fraction resulting from either outward flop of IL probe to the OL where it is quenched or the inward leak of dithionite to destroy intracellular probe. Thus, the DT quench data provide an independent estimate of the size of the OL pool for NBD-PE and NBD-PC. The kinetics of DT quench of NBD-PS are more complex. Following an initial decrease in fluorescence after DT addition, cell NBD-PS fluorescence increases, before decreasing again. Such a phenomenon has not been observed in cuvette studies of NBD-PS by DT and would compromise interpretation of cuvette measurements. Flow cytometry readily reveals this anomalous behavior but does not provide a simple means for detailed analysis and quantitative interpretation. Further examination of this behavior is required.

Kinetics of Phospholipid Transbilayer Movement. Flop Kinetics. The above reasoning is employed to derive the kinetic features of NBD-phospholipid flop from the BSA extraction experiments. In the case of NBD-PC, the majority of cellular probe is extracted in a single kinetic phase with a calculated $T_{1/2}$ of 108 s. This is taken to represent the rate of desorption of NBD-PC from the PM OL to acceptor in solution (BSA). Nearly complete quenching of NBD-PC by DT confirms the existence of a single pool in the PM OL. The kinetics of extraction of NBD-PE and NBD-PS are best fit by double-exponential equations. The most straightforward interpretation of these data is that the initial rapid phase represents extraction of OL probe, while the slower second phase represents extraction of IL probe which must first move (flop) to the OL. Other explanations for the slowly extracted fractions are possible. The surface of the bull sperm is heterogeneous with respect to both structure and function. Complete protein and lipid mixing (as measured by fluorescence recovery after photobleaching) do not occur from region to region of the sperm cell surface (Cardullo & Wolf, 1990), and gel phase domains may occur in the lipid phase of the PM under physiological condition (Wolf et al., 1990). Hence it is conceivable that some probe may be sequestered in a non- (or slowly) extractable pool in the OL. However, quenching of cell surface NBD-phospholipids by DT indicates that any such OL pools are not significant in size.

Flip Kinetics. The measurement of the rates of phospholipid flip across the PM requires knowledge of the total cellular and OL fluorescent probe and is limited by the time required to make a measurement of cell associated probe. The high throughput of the flow cytometer makes rapid determination of total cellular probe and total minus OL probe possible. The head group specificity of movement of NBD-phospholipids to a nonextractable pool (Figure 3) points to the action of the aminophospholipid translocase. The observed kinetics actually reflect the sum of inward and outward movement plus any movement to internal membranes. The contribution of outward movement (flop) of probe from the PM IL to the OL during the assay can be evaluated from the BSA extraction kinetics (Table 1).

Role of the Flippase in the Regulation of Sperm Cell Function. The inhibitor sensitivity of sperm transbilayer NBD-PL movement is similar to that reported for this activity in other cell types. Sensitivity of the flippase to cellular ATP levels is of special interest, since sperm cells have a uniquely simplified metabolism which has been characterized in detail (Hammerstedt et al., 1988). The apparent ubiquity of the aminophospholipid translocase in mammalian cells suggests this activity is an important housekeeping function, with a measurable metabolic cost. Hammerstedt et al. (1988) calculated that 3 μmol of ATP/(h·10^8 sperm) was consumed by unknown processes not related to motility, ion movement, or substrate cycling. The translocation of 50 pmol of NBD-PS by 1×10^7 cells with a half-time of approximately 2 min corresponds to an ATP consumption rate of 15 nmol of ATP/(h·10^8 sperm), assuming 1 ATP hydrolyzed/transloca-

tion. This estimate is based on a subsaturating challenge of exogenous substrate introduced into the OL and represents a minimal estimate. Substrate saturation of the translocase by trace probe is probably limited by the amount of exogenous lipid which can be inserted into the PM OL. Endogenous membrane lipid would already be at equilibrium, so the rate of inward phospholipid pumping would be dictated by the movement of substrate from the IL back to the OL. The surface area of a bull sperm cell has been measured to be 145 μm^2 (Drevius et al., 1972) and the protein/phospholipid of the anterior head PM is 0.66 (Parks et al., 1987). Assuming this value applies to the entire sperm plasma membrane and that mass is distributed equally between the two membrane leaflets, the total phospholipid surface area on both leaflets of the PM is approximately 174 μm^2. Further assuming an average surface area of 0.6 nm^2/phospholipid molecule on the bilayer, this amounts to approximately 2.9×10^8 molecules, 14% of which are aminophospholipids (Parks et al., 1987). Since the appearance of these 2.3×10^7 aminophospholipid molecules on the outer leaflet is dictated by the rate of flop (measured here to be approximately 0.0025 s^{-1}), we estimate aminophospholipids appear on the outer leaflet at a rate of 58 000 s^{-1}. If the flippase is always active to move PM outer leaflet PE and PS back to the IL, this would consume 38 nmol of ATP/($h \cdot 10^8$) sperm, assuming 1 ATP hydrolyzed/translocation. This order of magnitude calculation indicates that the activity of the flippase might account for 1% of the sperm cell's unidentified ATP consumption.

Control of flippase activity by physiological molecules (ATP and Ca^{2+}) is also of interest from the standpoint of regulation of sperm membrane function. Prior to fertilization, sperm cells must reside in the female tract for a period of time (Chang, 1951; Austin, 1952). During this time sperm undergo changes in metabolism and membrane structure, leading to a decrease in membrane stability. Membrane destabilization is a prerequisite for membrane fusion of the acrosome reaction and fertilization. In vitro studies suggest that these changes include alterations in sperm energy metabolism (Yanagamachi, 1988), an increase in sperm membrane Ca^{2+} permeability (Triana et al., 1980), and an efflux of cholesterol from the PM (Ehrenwald et al., 1988). Cholesterol depletion would be expected to increase the rate of transbilayer phospholipid movement (Morrot et al., 1989). This would increase ATP consumption, drain cell ATP reserves, and ultimately decrease the activity of the flippase. During residence in the female tract, sperm cells also experience a rise in intracellular [Ca^{2+}] (Yanagamachi, 1988), due to an increase in PM Ca^{2+} permeability, slowing of the outward Ca^{2+} pump (due to ATP depletion) or both. A rise in intracellular [Ca^{2+}] would inhibit flippase activity. A loss of plasma membrane asymmetry due to inhibition of the flippase would result in the appearance of PC on the PM IL. Sperm PM PC is characterized by highly unsaturated acyl chains (Parks & Hammerstedt, 1985; J. Parks, personal communication) and as PC accumulates on the IL, bilayer destabilization may occur. The synergistic effects of transbilayer lipid movement and cholesterol depletion may combine to prepare the PM IL for the fusion of the acrosome reaction. Thus, in this hypothetical scenario, the active flippase maintains a stable bilayer, and inhibition of the flippase and loss of asymmetry destabilizes the PM to allow membrane fusion.

Conclusions and Limitations to These Studies. The ability of flow cytometry to provide a direct measurement of cell associated probe is a major advantage of this method. The kinetic capabilities of the flow cytometer were employed to follow probe movement within and between cell membranes. These results were used to formulate a model of probe equilibria which was used to estimate the rate constants for NBD-phospholipid movement in cells.

Flow cytometry is a powerful tool for making measurements of cell fluorescence. The ability to make multiparameter fluorescence measurements of individual cells with discrimination between free and cell-bound probe provides numerous advantages over bulk fluorescence measurements of cell suspensions in cuvettes. Since flow cytometry rapidly (thousands of cells per second) measures the total cell fluorescence without any spatial resolution, the use of quantitative microscopic imaging will provide a valuable complementary technique, offering lower throughput but substantial spatial resolution. Such an approach will be especially useful in a cell type such as the sperm cell, which has several geographically distinct structural and functional surface domains.

Transbilayer phospholipid distribution is a complex phenomenon. Recently, Brumen et al. (1993) presented a comprehensive model of phospholipid movements, incorporating active and passive transport as well as mass balance considerations, and used it to simulate phospholipid movements in the erythrocyte. Here, we use a simple model to help interpret phospholipid movements in a cell with more complex membrane structure. Computer modeling of composite data of NBD-PL incorporation and extraction (Figure 6) by simultaneous differential equations fit the experimental data well while suggesting the need for the following refinements in our model and methods. First, NBD-PL incorporation into cells is clearly not a simple first-order process. Rather it is part of a complex equilibria between cell bound and extracellular probe, unique for each lipid tested, and cannot be experimentally manipulated to dissect individual components. Second, estimates of the rate constant of the first phase of probe extraction by BSA had larger coefficients of variation than estimates of the slower rate. This is likely due to errors associated with (a) the small amplitude of the first phase, (b) the rapid rate of this phase relative to time needed for sample mixing and introduction into the flow cytometer ($\approx$20 s) which limits the number of early time points obtained, and (c) the subtraction of background signal determined in cells treated with BSA only (which increases rapidly during this early phase). Finally, as described in the Brumen model for erythrocyte phospholipid movements, active transport by the flippase is only one of several possible pathways for lipid transbilayer diffusion in cell membranes. Passive transporters and spontaneous phospholipid movements may also play important roles in determining transbilayer phospholipid distribution.

Interpretation of the rates of fluorescent phospholipid movement is limited by consideration of the structural and physical similarities between the fluorescent analogue and endogenous lipids. For instance, it is conceivable that the short chain species tested here have a higher spontaneous (passive) transbilayer movement or a reduced affinity for the translocase enzyme. However, within those limits the experimental approach of determination of kinetic parameters coupled with computer simulation offers a powerful tool to

explore lipid dynamics in intact cells. Improved mixing capabilities for flow cytometry can decrease mixing times by an order of magnitude compared to those reported here. If employed in a simpler cell with no internal membrane (i.e., the erythrocyte), this approach should allow direct access to the mechanistic issues of (a) the passive, facilitated, and active movement of lipids, (b) the role of ATP (intra- or extracellular) in flip and flop, and (c) the origin of flippase inhibition by Ca^{2+} or sulfhydryl reagents. Further, interpreted within the limits of the similarities of fluorescent analogues to naturally occurring lipid species, kinetic information derived with these methods will enable predictions to be made about the transbilayer dynamics of endogenous phospholipids in live cells.

ACKNOWLEDGMENT

We thank Elaine Kunze for assistance with the flow cytometry and Joshua Colvin for help with computer programming.

REFERENCES

Austin, C. R. (1952) *Nature 170,* 326−328.
Bearer, E. (1991) *J. Electron Microsc. Tech. 16*, 281−297.
Brumen, M., Heinrich, R., Herrmann, A., & Müller, P. (1993) *Eur. Biophys. J. 22*, 213−223.
Calvez, J.-Y., Zachowski, A., Herrmann, A., Morrot, G., & Devaux, P. F. (1988) *Biochemistry 27*, 5666−5670.
Cardullo R. & Wolf, D. (1990) in *Ciliary and Flagellar Membranes* (Bloodgood, R., Ed.) Plenum Press, New York.
Chang, M. C. (1951) *Nature 168*, 697−698.
Chattopdhyay, A. (1990) *Chem. Phys. Lipids 53*, 1−15.
Colleau, M., Herve, P., Fellman, P., & Devaux, P. F. (1991) *Chem. Phys. Lipids 57*, 29−37.
Connor, J., & Schroit, A. J. (1988) *Biochemistry 29*, 37−43.
Devaux, P. F. (1991) *Biochemistry 30*, 1163−1173.
Drevius, L. O. (1972) *J. Reprod. Fertil. 28*, 29−39.
Ehrenwald, E., Parks, J. E., & Foote, R. H. (1988) *Gamete Res. 20*, 145−157.
Ferrell, J. E., Lee, K.-J., & Huestis, W. H. (1985) *Biochemistry 24*, 2849−2857.
Hammerstedt, R. H., Volante, C., & Racker, E. (1988) *Arch. Biochem. Biophys. 266*, 111−123.
Herrmann, A., & Muller, P. (1986) *Biosci. Rep. 6*, 185−191.
Hiipakka, R. A. & Hammerstedt, R. H. (1978) *Biol. Reprod. 19*, 368−379.
Homan, R., & Pownall, H. J. (1988) *Biochim. Biophys. Acta 938*, 155−166.
Juneja, L. R., Kazuoka, T., Goto, N., Yamane, Y., & Shimizu, S. (1989) *Biochim. Biophys. Acta 1003*, 277−283.
King, M., & Marsh, D. (1987) *Biochemistry 26*, 1224−1231.
Kobayashi, T., & Arakawa, Y. (1991) *J. Cell Biol. 113*, 235−244.
Koval, M., & Pagano, R. E. (1989) *J. Cell Biol. 108*, 2169−2181.
Martin, O. C., & Pagano, R. E. (1987) *J. Biol. Chem. 262*, 5890−5898.
McIntyre, J. C., & Sleight, R. G. (1991) *Biochemistry 30*, 11819−11827.
McLean, L. R., & Phillips, M. C. (1981) *Biochemistry 20*, 2893−2900.
Middlekoop, E., Lubin, B. H., Op den Kamp, J. A. F., & Roelofsen, B. (1986) *Biochim. Biophys. Acta 85*, 5421−5424.
Morrot, G., Herve, P., Zachowski, A., Fellman, P., & Devaux, P. F. (1989) *Biochemistry 28*, 3456−3462.
Müller, K., Pomorski, T., Müller, P., Zachowski, A., & Herrmann, A. (1994) *Biochemistry 33*, 9968−9974.
Nolan, J. P., Graham, J. K., & Hammerstedt, R. H. (1992) *Arch. Biochem. Biophys. 292*, 311−322.
Parks, J. E., Arion, J., & Foote, R. H. (1987) *Biol. Reprod. 37*, 1249−1258.
Seigneuret, M., & Devaux, P. F. (1984) *Proc. Natl. Acad. Sci. U.S.A. 81*, 3751−3755.
Struck, D. S., & Pagano, R. E. (1980) *J. Biol. Chem. 255*, 5404−5410.
Sune, A., Vidal, M., Morin, P., Sainte-Marie, J., & Bienvenue, A. (1988) *Biochim. Biophys. Acta 946*, 315−327.
Triana, L. R., Babcock, D. F., Lorton, S. P., First, N. L., & Lardy, H. A. (1980) *Biol. Reprod. 23*, 47−59.
Williamson, P., Kulick, A., Zachowski, A., Schlegel, R. A., & Devaux, P. F. (1992) *Biochemistry 31*, 6355−6360.
Wolf, D. E. (1987) *Ann. N.Y. Acad. Sci. 513*, 247−261.
Wolf, D. E., Maynard, V. M., McKinnon, C. A., & Melchoir, D. L. (1990) *Proc. Natl. Acad. Sci. U.S.A. 87*, 6893−6896.
Yanagamachi, R. (1988) in *The Physiology of Reproduction* (Knobil, E., & Neill, J., Eds.) Raven Press, New York.

BI941939Y